

Supplementary Material

On the impact of the stress situation on the optical properties of WSe₂ monolayers under high pressure

A Francisco-López,¹ B Han,² D Lagarde,² X Marie,² B Urbaszek,² C Robert,² A R Goñi^{1, 3*}

¹ Institut de Ciència de Materials de Barcelona (ICMAB-CSIC), Campus de la UAB, 08193 Bellaterra, Spain.

² Université de Toulouse, INSA-CNRS-UPS, LPCNO, 135 Avenue de Rangueil, 31077 Toulouse, France.

³ ICREA, Passeig Lluís Companys 23, 08010 Barcelona, Spain.

I. PL measurements under pressure

Figures 1a-d show the pressure dependence of PL peak energy and intensity, resulting from least-squares fits to the spectra of the bare WSe₂ ML and the hBN/WSe₂-ML/hBN heterostructure sample using a Gaussian-Lorentzian cross-product function. As explained in the main text, this PL peak is associated to radiative recombination of the A-exciton, which involves direct (only for a ML) optical transitions at the K points of the Brillouin zone. In the figures, the acquisition sequence for the data point is indicated: i) First a downstroke from the initial pressure obtained right after closing the DAC, ii) followed by the main pressure upstroke in small steps, and iii) the final downstroke to test reversibility of pressure-induced changes.

As discussed in the main text, the pressure-induced change in the A-exciton energy exhibits a different sign for both samples, which is believed to

be due to a distinct stress situation. The PL intensity, however, displays in both cases a monotonic reduction with increasing pressure. The reduction is reversible, provided the pressure does not exceed a value of about 11 GPa. In this case, the data of Figs. 1a,b indicate that the PL emission energy recovers but not the PL intensity. This might be the consequence of formation of structural defects that lead to PL quenching, which are precursors of the occurrence of a structural phase transition above but close to 13 GPa.

II. PLE measurements under pressure

Representative PLE spectra (closed symbols) are displayed in Figs. 2(a,b) for the case of the bare WSe₂ ML and the hBN-encapsulated WSe₂ ML sample, respectively. Each data point of each PLE spectrum corresponds to the energy of the tunable laser used for excitation and the integrated intensity of the A-exciton PL peak, normalized by the incident laser power at the tuned wavelength. The PLE spectra exhibit essentially two features: a kind of excitonic absorption edge associated with the B-exciton and a peak-like feature corresponding to a high-energy critical point (CP) in the joint density of states of a WSe₂ ML [1]. Changes in the PLE lineshapes under pressure were analyzed using a fitting function (solid black curves in Figs. 2(a,b)) [2], which consists of two components. The CP feature

*E-mail: goni@icmab.es

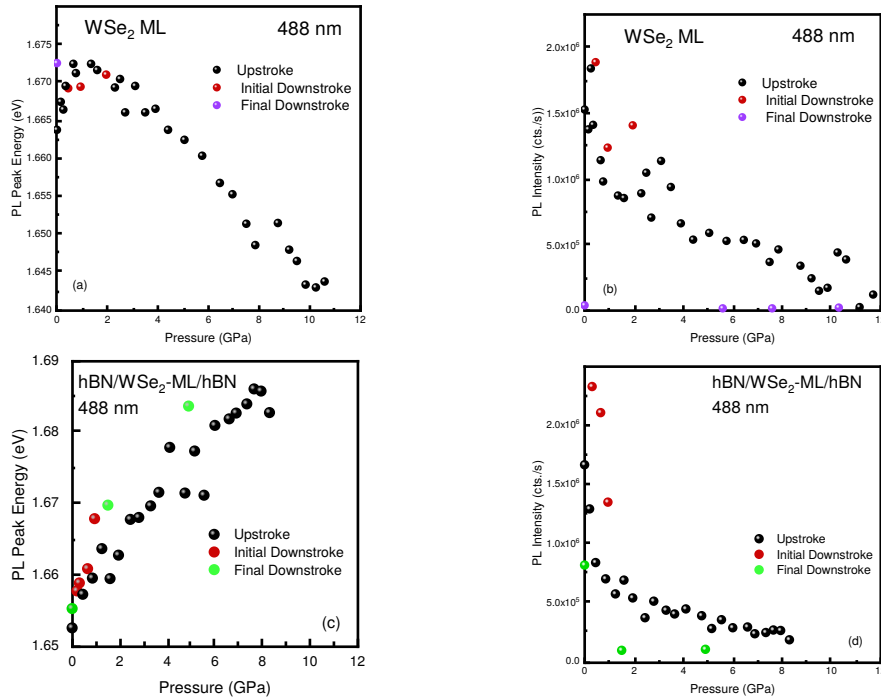


Figure S 1: Room-temperature PL peak energy and intensity of the A-exciton as a function of pressure (a),(b) for the bare WSe₂ ML and (c),(d) for the hBN/WSe₂-ML/hBN vdW heterostructure. The PL was excited with the 488 nm line.

could be well described by a Gaussian, whereas for the B-exciton we considered a series of Gaussian peaks accounting for the discrete energy spectrum [3] and the analytical expression derived for the exciton continuum in Ref. [4]. The peak at around 2.35 eV for the hBN-encapsulated WSe₂ ML sample is most likely a spurious signal, because its energy does not depend on pressure at all. A similar peak is also observed in the PLE spectra of the bare WSe₂ ML but it is so weak that is not taken into account when fitting the PLE profiles. Its origin is still elusive.

Figures 3a,b show the peak energy values of the CP feature as a function of pressure, as obtained from lineshape fits to the PLE spectra. Interestingly, the pressure dependence of this high-energy CP feature differs from the one of the A,B-excitons, indicating that higher excited states react different upon compression. Furthermore, the change of the CP energy under pressure is also different for the bare and the encapsulated WSe₂ ML sample. For

the bare ML the CP feature energy exhibits a non-monotonic behavior with an initial increase, as the A,B-excitons, followed by a turn over and a final decrease. For the encapsulated ML, however, the CP energy decreases linearly with pressure at a rate of -4.6 meV/GPa.

III. On the stress/strain situation of 2D systems inside the DAC

In order to correctly address adhesion effects and the possible transfer of strain from the substrate, the diamond anvil in our case, either to the single WSe₂ monolayer (ML) or to the hBN/WSe₂-ML/hBN sandwich we ought to discuss two key points: 1) The difference in the elastic properties between graphene and a WSe₂ ML, in particular, or transition metal dichalcogenide MLs, in general. 2) The different stress-strain situation that arises if the sample under study is supported by a Si/SiO₂ substrate (with a thick silicon oxide layer) or if it

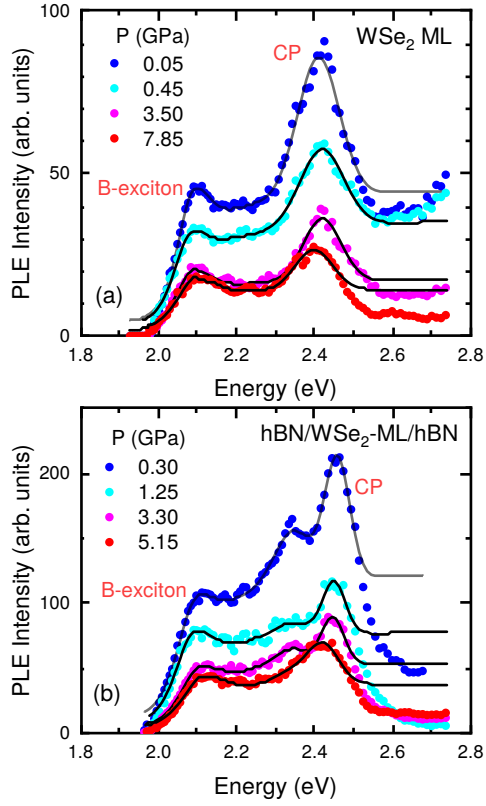


Figure S 2: PLE spectra (closed symbols) of (a) the bare WSe_2 ML and (b) the $\text{hBN}/\text{WSe}_2\text{-ML}/\text{hBN}$ heterostructure sample at different pressures, as indicated. The solid black curves represent the lineshape fitting function associated to the B-exciton and a critical point (CP).

was directly transferred onto one of the diamond anvils, as is our case.

1) **WSe_2 ML versus graphene:** It is a common practice to write the fourth-rank tensor corresponding to the elastic stiffness constants C_{ijkl} in form of a 6×6 matrix which relates the stress and strain tensors σ_{ij} and ϵ_{kl} (written as 1×6 vectors), respectively, as:

$$\sigma_i = C_{ij} \cdot \epsilon_j, \quad i, j = 1, \dots, 6. \quad (1)$$

For a 2D system with isotropic in-plane elastic properties (x, y plane) and completely neglecting shear stress components, C_{ij} becomes a 3×3 ma-

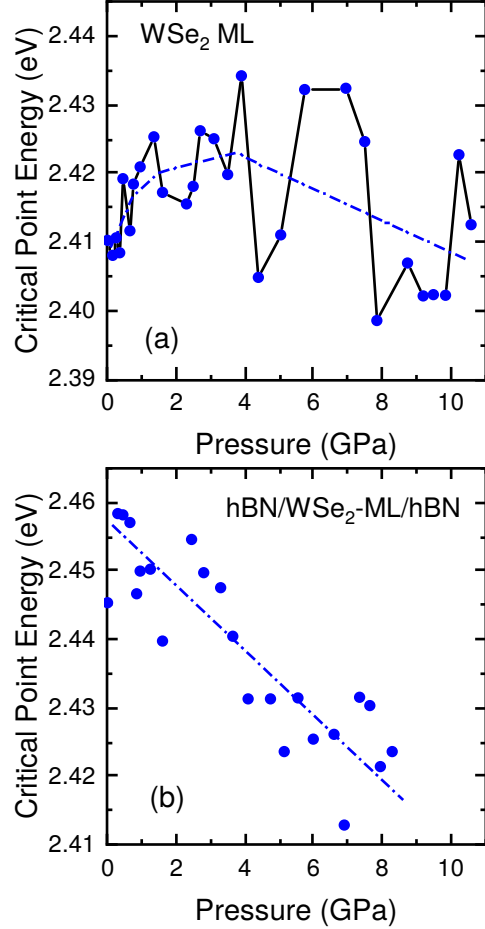


Figure S 3: Peak energy of the critical point (CP) feature in PLE spectra, as extracted from lineshape fits, plotted as a function of pressure (a) for the bare WSe_2 ML and (b) for the $\text{hBN}/\text{WSe}_2\text{-ML}/\text{hBN}$ vdW heterostructure. Lines are a guide to the eye.

trix of the form:

$$C_{ij} = \begin{pmatrix} C_{11} & C_{12} & C_{13} \\ C_{12} & C_{11} & C_{13} \\ C_{13} & C_{13} & C_{33} \end{pmatrix}, \quad (2)$$

where we adopted z as the out-of-plane direction. Let us consider the case of a uniaxial stress X in the out-of-plane direction, i.e. $\sigma = (0, 0, X)$. Using Eqs. (1) and (2), the out-of-plane and in-plane strain components induced by the uniaxial stress X

are readily obtained as

$$\begin{aligned}\epsilon_z &= \frac{C_{11} + C_{12}}{C_{33}} \cdot \frac{X}{D} \\ \epsilon_{xy} &= -\frac{C_{13}}{C_{33}} \cdot \frac{X}{D},\end{aligned}\quad (3)$$

with $D = C_{11} + C_{12} - 2\frac{C_{13}^2}{C_{33}}$. A compressive stress X perpendicular to the layer thus gives rise to a tensile in-plane strain proportional to X .

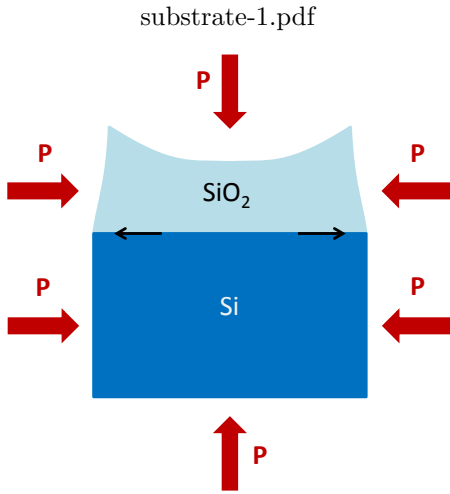


Figure S 4: Schematic view of the deformations induced by the hydrostatic compression of a Si/SiO₂ substrate in the DAC.

Precisely in this respect, the elastic behavior of a single graphene sheet is qualitatively different from that of a single monolayer of any transition-metal dichalcogenide (TMD). Being graphene a truly 2D system consisting of an absolutely planar monatomic layer and provided that the atomic wavefunctions can be considered as incompressible, hence, to a very good degree of approximation the out-of-plane related stiffness constants become $C_{33} \rightarrow \infty$ and $C_{13} \rightarrow 0$. Inspection of Eqs. (3) reveals that both strain components vanish ($\epsilon_z, \epsilon_{xy} \rightarrow 0$), which means that an uniaxial out-of-plane stress has no effect at all upon the graphene layer. This apparently minor result has important consequences for the elastic response of graphene under high hydrostatic pressure conditions like in experiments with the diamond-anvil cell: If, as we

propose in this paper, the pressure medium is unable to exert any in-plane pressure, due to the vanishing lateral area exposed by a single atomic layer, then the only way to deform single-layer graphene is through the effect of the substrate, as discussed elsewhere (see Refs. [5, 6] and references therein).

In contrast, monolayers of TMDs like WSe₂ consist of three covalently bonded atomic layers (Se-W-Se in our case). As a consequence, the elastic stiffness tensor of a TMD ML is that of a 3D object with a finite $C_{33} \approx C_{11} \approx 120$ GPa and non-vanishing $C_{13} \approx C_{12} \approx 30$ GPa [7] (here we considered the all tetrahedrally bonded monolayer well behaving as a cubic solid, whereas the bulk possesses much lower values of the out-of-plane related stiffness constants due to the much weaker vdW interlayer bonding). According to Eqs. (3), this means that a uniaxial compressive stress in the out-of-plane direction would cause a tensile in-plane deformation which, being mediated by purely covalent forces, would be always stronger than any possible strain transferred from the substrate through vdW adhesion forces! We can foresee only one exception, occurring for Si/SiO₂ substrates, as discussed next.

2) **Si/SiO₂ substrate:** Almost all high pressure experiments performed on monolayers of TMD materials were carried out with the 2D sample supported by a pretty thick (about 300 nm) SiO₂ layer on top of a Si substrate. To understand the behavior of the TMD ML in high pressure experiments is imperative to perform an analysis of the elastic deformations suffered by the Si/SiO₂ substrate under compression in the DAC. The key point is that the bulk modulus of the amorphous silicon dioxide (33.5 - 36.8 GPa [9]) is about one third of that of crystalline Si (98 GPa [8]), i.e., the SiO₂ layer is roughly three times more compressible than the silicon. Under high hydrostatic pressure the whole substrate would be deformed as sketched in Fig. 4: With increasing pressure, the much thicker but less compressible Si would exert a tensile stress on the oxide layer, which induces a contraction of the SiO₂ layer in out-of-plane direction. This tensile in-plane stress, which only acts at the interface between Si and the oxide, relaxes simultaneously towards the upper and the lateral surfaces of the 300 nm-thick oxide layer, the ones which are being compressed by the pressure medium. As illustrated in Fig. 4, the result is the formation of a concave surface onto which the TMD ML is pressed against by

the pressure transmitting medium. In this case, we anticipate a complicated, non-uniform, substrate-induced strain situation for the 2D system, despite the hydrostatic conditions ensured by the pressure transmitting medium.

In principle, the surface of the diamond anvil would also develop a concave curved surface when the DAC is pressurized. Nevertheless, because of the extremely high bulk modulus of diamond (560 GPa [8]), the curvature of the diamond surface would be about one order of magnitude smaller than for the Si/SiO₂ substrate. We are thus confident that the diamond can be left out of the discussion of the stress/strain situation of our 2D systems, which were directly transferred onto one of the anvils of the DAC.

IV. Raman measurements under pressure

The Raman modes are quite sensitive to strain. The out-of-plane A₁' vibration ought to be sensitive to strain in perpendicular direction to the ML [10]. The two upper panels of Fig. S5 show the Raman spectra measured with 785 nm excitation for the bulk and the encapsulated WSe₂ ML as a function of pressure, corresponding to the data of Fig. 6a of the main manuscript. Again, due to resonance effects, with IR excitation (785 nm) the dominant peak in Raman spectra in the range of 250 cm⁻¹ corresponds to the A_{1g} (A₁') in bulk (ML) WSe₂. As demonstrated in the manuscript, both modes exhibit, within experimental uncertainty, the same pressure dependence. This is compatible with the assumption that the encapsulated ML is hydrostatically compressed in the DAC (hydrostatic stress situation).

The two lower panels of Fig. S5 show the corresponding Raman spectra measured with blue (488 nm) excitation for the encapsulated and the bare WSe₂ ML taken at different pressures and corresponding to the data of Fig. 6b of the main manuscript. In contrast, with blue excitation the most prominent feature in the Raman spectra corresponds to the doubly degenerate E' modes, for which the atomic displacements are in plane. As shown in the manuscript, the E' mode of the bare ML exhibits a smaller pressure coefficient, as compared to the coefficient of the same mode for the

encapsulated ML. A ratio of approx. 1.3 is obtained for the pressure coefficient of the E Raman modes for the case of WSe₂ ML encapsulated in hBN relative to that of the bare ML on diamond. As explained above, if we assume that the encapsulated ML is subjected to a fully hydrostatic compressive stress, the lower slope of the E' modes of the bare ML speaks for an uniaxial stress situation along the direction perpendicular to the plane of the bare ML. Theoretically, for pure uniaxial stress the ratio of pressure coefficient of the hydrostatic component and that of the doublet (the E modes in this case) amounts to 1.5 [11], very close to the value determined here.

-
- [1] A Carvalho, R M Ribeiro, A H Castro Neto, *Band nesting and the optical response of two-dimensional semiconducting transition metal dichalcogenides*, Phys. Rev. B **88**, 115205 (2013).
 - [2] M. Wojdyr, *Fityk: a general-purpose peak fitting program*, J. Appl. Cryst. **43**, 11261128 (2010).
 - [3] M Brotons-Gisbert, A Segura, R Robles, E Canadell, P Ordejón, J F Sánchez-Royo, *Optical and electronic properties of 2H-MoS₂ under pressure: revealing the spin-polarized nature of bulk electronic bands*, Phys. Rev. Mater. **2**, 054602 (2018).
 - [4] A R Goñi, A Cantarero, K Syassen, M Cardona, *Effect of Pressure on the Low-Temperature Excitonic Absorption in GaAs*, Phys. Rev. B **41**, 10111-10119 (1990).
 - [5] Machon, D.; Bousige, C.; Alencar, R.; Torres-Dias, A.; Balima, F.; Nicolle, J.; Pinheiro, G. S.; Souza Filho, A. G.; San-Miguel, A. Raman scattering studies of graphene under high pressure. *J. Raman Spectrosc.* **2018**, 49, 121.
 - [6] Bousige, C.; Balima, F.; Machon, D.; Pinheiro, G. S.; Torres-Dias, A.; Nicolle, J.; Kalita, D.; Bendiab, N.; Marty, L.; Bouchiat, V.; Montagnac, G.; Souza Filho, A. G.; Poncharal, P.; San-Miguel, A. Biaxial strain transfer in supported graphene. *Nano Lett.* **2017**, 17, 21-27.

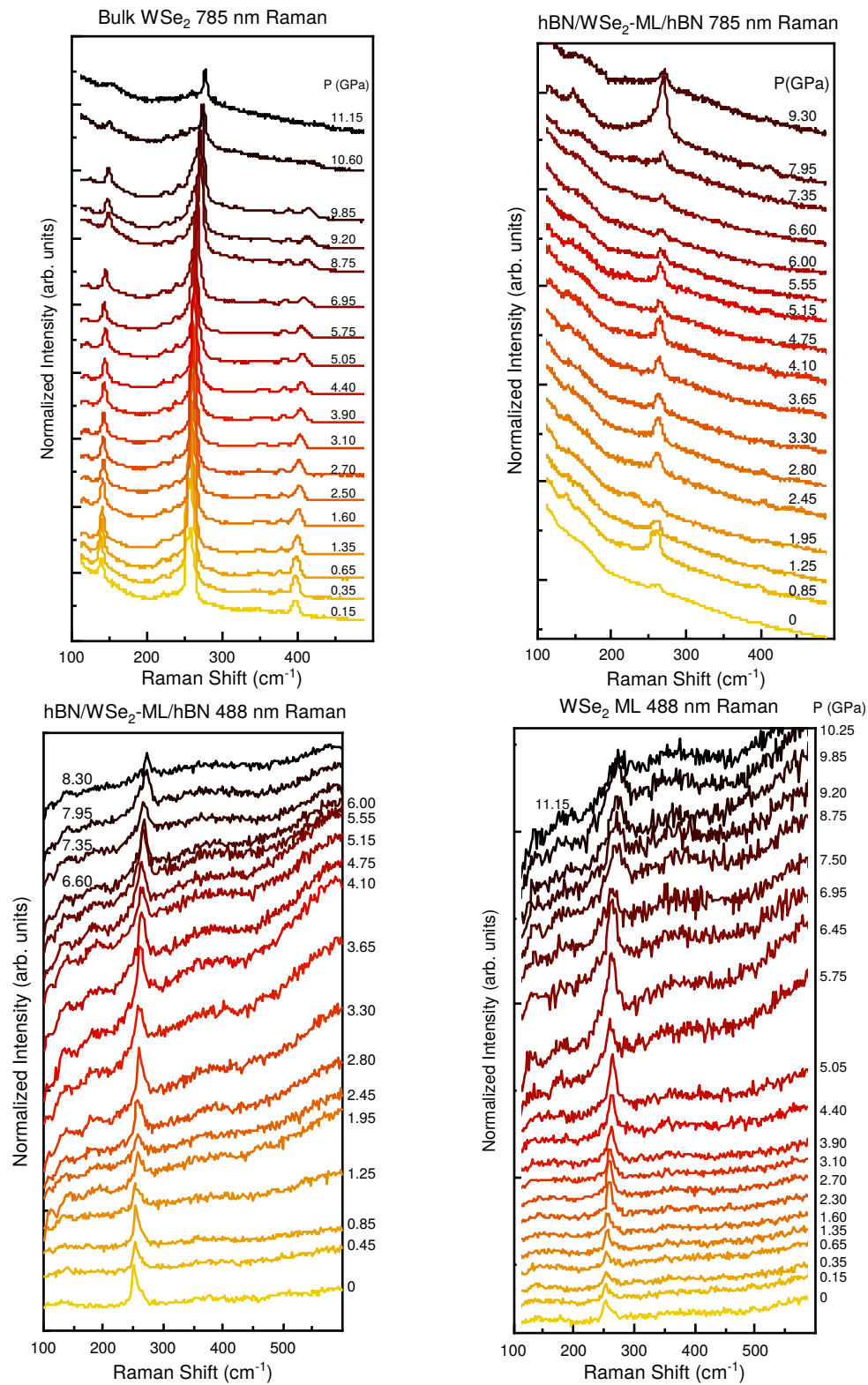


Figure S 5: Representative room-temperature Raman spectra as a function of pressure, corresponding to the cases associated with the data plotted in Figs. 6a,b of the manuscript. (Upper left panel) and (upper right panel) Raman spectra of bulk WSe_2 and the encapsulated WSe_2 ML, respectively, measured with IR excitation (785 nm). (Lower left panel) and (lower right panel) Raman spectra of the encapsulated and bare WSe_2 ML, respectively, excited with the 488 nm line.

- [7] L-P Feng, N Li, M-H Yang, Z-T Liu, *Effect of pressure on elastic, mechanical and electronic properties of WSe₂: A first-principles study*, Mater. Res. Bull. **50**, 503508 (2014).
- [8] *Numerical Data and Functional Relationships in Science and Technology*, Vol. 17a of *Landolt-Börnstein*, New Series, ed. Madelung, O.; Weiss, H.; Schulz, M. (Springer, Heidelberg, 1982).
- [9] <https://www.azom.com/properties.aspx?ArticleID=1114>
- [10] B Han, F Li, L Li, X Huang, Y Gong, X Fu, H Gao, Q Zhou, T Cui, *Correlatively dependent lattice and electronic structural evolutions in compressed monolayer tungsten disulfide*, J. Phys. Chem. Lett. **8**, 941-947 (2017).
- [11] E Anastassakis, M Cardona, *Phonons, strains, and pressure in semiconductors*, Semicond. Semimetals **55**, 117-233 (1998).